Modelling of down-draft gasification of biomass – an integrated pyrolysis, combustion and reduction process

Chidiebere Diyoke [a], Ningbo Gao [b*], Mathew Aneke[c], Meihong Wang [c*], Chunfei Wu [a*],

[a] School of Engineering, University of Hull, Hull, UK, HU6 7RX.

[b] School of Energy and Power Engineering, Xi'an Jiaotong University, Xi'an, China, 710049.

[c] Department of Chemical and Biological Engineering, University of Sheffield, UK S1 3JD

Tel/Fax: +44-1482 466464; E-mail: c.wu@hull.ac.uk (C Wu); Meihong.Wang@sheffield.ac.uk (M Wang); nbogao@xjtu.edu.cn (N Gao);

Abstract

A gasification model is developed and implemented in Matlab to simulate a downdraft gasifier using wood as feedstock. The downdraft gasifier was conceptually divided into three zones: the pyrolysis zone, the combustion/oxidation zone and the reduction zone. A typical tar composition and its mole fraction, as reported in the literature was supplied as an input parameter in the model. The concentration of syngas and profiles of temperature along the reduction zone length were obtained by solving the mass and energy balances across each control volume and taking into account the rate of formation/consumption of the species according to different gasification kinetics. The simulation results from the model agreed closely with the experimental results. The syngas concentration was found to be about 1.1%, 17.3%, 22.8%, 9.0% and 49.8% for CH_4, H_2, CO, CO_2, and N_2 respectively and the corresponding LHV, CGE, CCE and yield were 4.7 MJ/Nm^3, 59.9%, 85.5% and 2.5 Nm^3/kg-biomass respectively at ER of 3.1 and fuel moisture content of 18.5% wt. Sensitivity analysis was carried out with this validated model for different air-fuel ratios, moisture contents and inlet air temperature. The analysis can be applied to produce specific design data for a downdraft biomass reactor given the fuel composition and operating conditions.

Key words: Gasification, Downdraft gasifier; modelling, Biomass, Performance analysis,

Nomenclature

a	specific heat constant ($Jmol^{-1}K^{-1}$)	**subscript**	
b	specific heat constant ($Jmol^{-1}K^{-1}$)	B	Biomass
C	Weight percent of carbon in fuel (%)	F	formation
E	Activation energy ($kJkmol^{-1}$)	i	oxidation product species
FF	Frequency factor for reaction(s^{-1})	j	Pyrolysis product species
$\dot{h}$	Molar specific enthalpy ($Jmol^{-1}K^{-1}$)	mc	No of atoms of carbon
$\dot{h}_{f,B}$	Heat of formation of biomass ($Jmol^{-1}K^{-1}$)	mh	No of atoms of hydrogen
H	Weight percent of hydrogen in fuel (%)	mo	No of atoms of oxygen
HV	Heating value (MJ/kg)	ox	oxidation
$\Delta\dot{h}_f$	Enthalpy of formation ($Jmol^{-1}$)	p	pyrolysis
$\Delta\dot{h}_v$	Heat of vaporization of moisture ($Jmol^{-1}$)	R	Reduction zone
k^0	Pre-exponential factor (s^{-1})	R	Reaction
MC	Fuel moisture content (% wt.)	w	moisture
Mm	Molar mass ($gmol^{-1}$)	x	Reaction number
n	No of moles or molar flow rate		
N	No of moles		
O	Weight percent of oxygen in fuel (%)		
P	Partial pressure (Pa)		
Q_{air}	Flow rate of air (m^3/s),		
Q_{dry}	Heat to dry away moisture ($Jmol^{-1}$)		
$Q_{l,p}$	Heat loss in pyrolysis zone ($Jmol^{-1}$)		
$Q_{l,ox}$	Heat loss in oxidation zone ($Jmol^{-1}$)		
R	Gas constant($Jmol^{-1}K^{-1}$)		
$r_{R,i}$	Rate of reaction ($molm^{-3}s^{-1}$) for i^{th} reaction		
Rt	Rate of production ($molm^{-3}s^{-1}$)		
v	Gas velocity (m/s)		
w	Amount of moisture (mol^{-1} of wood)		
y_i	molar ratio of the respective gases		
z	Reduction zone length (m)		

Abbreviations

CGE Cold gas efficiency
En Energy
ER Equivalent ratio
HV Heating value
MC Fuel moisture content
Mm Molar mass
Oz Oxidation zone
PZ Pyrolysis zone
RZ Reduction zone
Mm Molar mass

1. Introduction

The utilisation of fossil fuel, which accounts for over 75% of the world energy source, has been implicated as the main cause of global warming [1]. Within the last decade, there has been a growing concern towards global warming and the depletion of fossil fuels in the future [2]. To guarantee security of energy supply while reducing the carbon footprints of energy generation, the energy policy globally is shifting towards renewable based power generation. Among the renewables, biomass is one of the promising renewable energy sources of the future because they are largely available globally. Biomass is ranked the fourth highest primary energy resource globally after crude oil, coal, and gas, representing about 10.6% of the global primary energy supply [3].

Biomass energy is the most viable form of energy for developing countries [1, 4]. However, in the years past, the developed European countries have recognised the importance, biomass energy holds for their energy economy in terms of converting wastes to energy, chemicals and combined heat and power (CHP) applications [5]. Biomass is projected to contribute about 56% of the renewable energy supply in the EU27 by 2020 [5, 6]. Biomass can be converted to energy through combustion or gasification. Gasification of biomass has been suggested to be the most cost effective route to realize biomass energy [7]. It involves heating biomass to a high temperature in the range of 1500-1600 K in a reactor with oxygen less than the stoichiometric requirement for complete combustion of the fuel to form volatile compounds (gases) and solid residues (char) [8]. Numerous biomass gasification reactors have been designed including moving (fixed) bed, fluidized bed and entrained-flow gasifier [9-11].

In fixed bed reactors, the biomass feed travels either counter-current or co-current to the flow of gasification medium (steam, air or oxygen) as the fuel is converted to fuel gas [8, 9]. The fixed bed reactors are comparatively simple to operate and largely experience minimum erosion of the reactor body. There are three basic fixed bed designs – updraft, downdraft and cross-draft gasifiers [9]. Different from fixed bed reactors, fluidized bed gasifiers (bubbling or circulating) have no separate reaction zones and drying, pyrolysis and gasification happens concurrently during mixing. They are complicated and use expensive control systems. As a result, fluidized bed gasifiers tend to be commercially viable at bigger sizes (> 30 MW thermal output) [8, 9]. In an entrained-flow gasifier, the biomass fuel particle is fed into the gasifier from the top in a coaxial flow of the gasifying medium (oxygen and steam, in some instances, carbon dioxide or a mixture of them). They are usually operated at pressures of 20-70 bar and at a temperature around 1400 ºC. Tar production is negligible, since the gases released pass

through the very high-temperature (1000 °C) zone and are therefore nearly all converted into tar free syngas but with the penalty of oxygen consumption. Detailed analysis of the various types of gasifiers can be found in the literatures [9, 11, 12].

The downdraft gasification process possess several advantages. The synthesis gas leaves the gasifier from the end and carries significantly less tar than from updraft gasifier, which reduces the need for cleaning; making it more appropriate for a wider range of applications[9]. Although it has little flexibility for different feedstock, fuel moisture content and size, it is the technology for small-scale processes with electrical output not more than 500 kW_e [9]. Other advantages of downdraft gasifier include simple design, very good carbon conversion, low capital cost and good compatibility with internal-combustion engines [10]. Additionally, the time needed to ignite and bring the downdraft gasifier to working temperature is shorter (20-30 minutes) compared to the time required by an updraft gasifier [12].

Consequently, the downdraft gasification process has received considerable attention in the literature recently. Qualitative downdraft gasification models have been reported by Melgar et al. [13], Giltrap et al. [14], Morten, [15], Zainal et al. [4] and Babu et al. [16]. Sharma [17] carried out a comparison of equilibrium and kinetic modelling of char reduction reactions in a downdraft biomass gasifier. An equilibrium model for predicting the syngas composition in a downdraft gasifier fed by solid waste was developed by Jarungthammachote and Dutta [18]. Melgar et al. [13] predicted the reaction temperature and final syngas composition using a combination of chemical equilibrium and thermodynamic equilibrium approach. Experimental studies have been published by Sheth and Babu [19], Zainal et al. [20] , Jayah et al. [21], Sarker and Nielsen [22], and Ratnadhariya and Channiwala [23]. Sharma [24] experimentally obtained temperature profile, gas composition, calorific value and trends for pressure drop across a porous gasifier bed. Ratnadhariya and Channiwala [25] developed a detailed model of a three-zone equilibrium and kinetic free model of biomass gasification in a downdraft gasifier. Qualitative agreement with experimental data is established. In another study, Di Blasi [26] developed a comprehensive dynamic model for studying the behaviour of stratified downdraft gasifiers. Their results showed that the predictions of the gas composition are in agreement with experimental data.

Gao and Li [7] modelled the combined pyrolysis and reduction zone of a downdraft gasifier. Their model was made up of three parts: the pyrolysis, oxidation and reduction zone. In the model, it was assumed the products of pyrolysis were only CO, CH$_4$ and H$_2$O and only the pyrolysis and reduction zones were considered leaving out the combustion zone. The main

weakness of their model is the inability to predict gas concentrations at the two zones and the omission of H_2 and tar in the assumed pyrolysis gas. Hence, an improvement to the model is necessary to extend its application and make it more robust.

In this work, the prediction of the pyrolysis and oxidation zone temperature are included. The reactor consists of three zones; pyrolysis, combustion and gasification zone where different reactions take place. The method adopted by Ratnadhariya and Channiwala [25] is used in the estimation of the pyrolysis and oxidation product species. One of the differences between this model and Ratnadhariya and Channiwala's model is in the treatment of the water-gas shift reaction and tar. Ratnadhariya and Channiwala did not account for tar in the pyrolysis product composition and water gas shift reaction. Different from the work from Ratnadhariya et al., tar in the composition of syngas was considered in this work. According to Cho and Joseph, [27] water-gas shift reaction is catalysed by the mineral matter in coal. Extending this to biomass, kinetic equations for this reaction have been incorporated in the model as well.

Furthermore, energy and material balances around the pyrolysis and oxidations zones are applied with some simplifying assumptions to obtain a more accurate representation of the temperature in the various sections of the reactor. Then a parametric study of the effect of operating conditions and fuel properties on the cold gas efficiency, gas yield, heating value and carbon conversion efficiency was carried out.

2. Model development

The downdraft biomass gasifier under consideration is schematically shown in Figure 1. It consists of three distinct partitions where distinct chemical and physical events take place: heat up/drying/pyrolysis, combustion and gasification. Biomass fed into the reactor reacts with air/oxygen/steam at atmospheric pressure to generate fuel gases made up of mainly hydrogen and carbon monoxide and small amounts of methane.

At the pyrolysis zone, the dried biomass is first thermally cracked into volatile products (VPs1), char and active tar (Tar_{active}) in a primary reaction [28]. The VPs1 consist of the gases (CO, CO_2, CH_4, H_2 C_2H_4, and H_2O). The active tar simultaneously undergo secondary pyrolysis to yield secondary volatile products (VPs2) like CO, CO_2, H_2, some hydrocarbons like C_2H_6, C_2H_4, and C_3H_6, and inert tar [28, 29].

The products of the primary and secondary pyrolysis reactions make up the final pyrolysis product species. These species pass through the high temperature oxidation/combustion zone

where further reactions happen. These reactions occur very fast and release a large amount of heat, which provides the energy needed to sustain the endothermic gasification reactions [8]. To estimate the temperature profile of the various zones of the gasifier, energy and material balances were written for the thermochemical processes taking place in each section of the gasifier and with the aid of some simplifying assumptions, the molar concentration and temperature of the volatiles in each zone were determined.

2.1. Drying Zone

The temperature attained in a biomass gasifier is affected greatly by the moisture content of the raw biomass. The moisture content of fresh cut wood biomass is very high, ranges from 30 to 60 percent by weight (% wt.) [30, 31]. In order to produce a product gas with considerably high heating value, gasification system make use of biomass whose moisture have been reduced to the range of 5–20 % wt. [30]. In the drying zone, the moisture in the wet biomass is removed using the heat generated by the partial combustion of some part of the fuel wood in the combustion zone. To model the drying process, a simplified approach was adopted. The quantity of energy required to dry out moisture, Q_{dry} is the sum of the sensible heat (Q_s) required to heat moisture to drying temperature and the heat required to evaporate moisture (Q_{evap}):

$$Q_{dry} = w * \left[C_{p,w}(\Delta T) + \Delta \dot{h}_{v,w} \right] \tag{1}$$

Where w represents the amount of moisture per mol of wood, $C_{p,w}$ is the specific heat of water, ΔT is the temperature difference between the initial and final state of moisture in the wood and $\Delta \dot{h}_{v,w}$ is latent heat of vaporization of water.
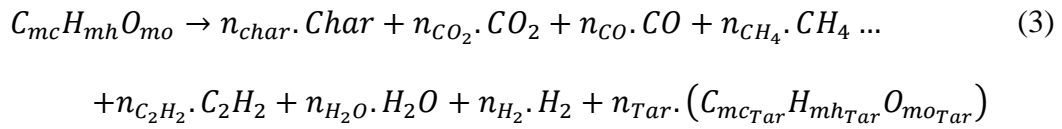
The amount of moisture per mol of wood was obtained as follows: [13].

$$w = \frac{Mm_B * MC}{Mm_{H_2O} * (1 - MC)} \tag{2}$$

Where Mm_B represents the molar mass of the biomass, MC is the biomass moisture content by weight and Mm_{H_2O} is molar mass of water.

2.2. Pyrolysis zone

In the pyrolysis zone, by means of the heat from the combustion zone, the biomass was first cracked down to primary pyrolysis products (gases and char) including primary tar [32]. According to Radmanesh et al. [33], 60% of the primary pyrolysis product accounts for primary tar. The primary tar compounds react further in a secondary reaction to yield volatiles (CO, CO_2, H_2, CH_4), heavier hydrocarbons $(e.g., C_2H_6, C_2H_4, C_3H_6)$ and inert tar [34] . The process is complicated involving complex reactions and it is difficult to capture all the complex reactions and their parameters in one model. In this work, rather than try to capture all the parameters, the most important parameters such as temperature, concentration and heating conditions were considered [35]. Using the above parameters, the overall pyrolysis process was modelled by the global one-step pyrolysis model reaction of Eq.3 [32].

$$C_{mc}H_{mh}O_{mo} \rightarrow n_{char}.Char + n_{CO_2}.CO_2 + n_{CO}.CO + n_{CH_4}.CH_4 \dots \qquad (3)$$

$$+n_{C_2H_2}.C_2H_2 + n_{H_2O}.H_2O + n_{H_2}.H_2 + n_{Tar}.\left(C_{mc_{Tar}}H_{mh_{Tar}}O_{mo_{Tar}}\right)$$

Where mc, mh and mo are the number of atoms of carbon, hydrogen and oxygen in the biomass, n is the number of moles of species of the respective pyrolysis product species and mc_{Tar}, mh_{Tar} and mo_{Tar} is the number of atoms of carbon, hydrogen and oxygen in the tar respectively.

The yields of the pyrolysis product species were estimated by forming a set of seven simultaneous equations, with the final mole of char and the six volatile matter species as unknowns. Predicting the specie of tars formed in pyrolysis reaction is challenging since the process involves very complex chemical reactions. Tar yield varies with the composition of biomass and temperature. In downdraft biomass gasification, maximum tar yield is negligible and does not vary much with temperature [36]. Hence for simplicity and since tar is a less important variable to be predicted, tar was considered as an input variable. Tar yield was assumed to have constant representative elemental composition of $CH_{1.03}O_{0.33}$ [37] with a maximum inert tar yield of 4.5% by mass as reported by the authors [37, 38] in their experiment

The first three equations are the elemental balance equations for carbon, hydrogen and oxygen respectively. The fourth and fifth equation are used to express water and hydrogen yield from the available oxygen and hydrogen in the biomass after tar formation respectively. It is assumed that 80 % of the available oxygen in the fuel is evolved in water formation in the pyrolysis zone [25, 39] while half of the available hydrogen after water and tar formation is evolved as

hydrogen gas [25]. The remaining two equations were used to express the molar yield of CO, CO_2 CH_4 and C_2H_2. The yield of the first two were related to the available oxygen content of the biomass after water and tar formation while the yield of the last two is related to the biomass hydrogen content. It is assumed the remaining oxygen is evolved in the formation of CO and CO_2 with the mole of the species formed related according to the inverse of their molar mass ratio [25, 40, 41].

The remaining hydrogen in the fuel is assumed to have evolved in the formation of CH_4 and C_2H_2 with the moles of each specie related according to the inverse ratio of their molar masses [25, 40, 42]. Other simplifying assumptions include the following:

- All the elemental hydrogen and oxygen in fuel is released during de-volatilisation; and hence the char formed is modelled as pure carbon [43, 44]

- Char yield in the gasifier is insensitive to pyrolysis temperatures encountered in the pyrolysis zone[43, 44]

- Temperature of the volatiles is the same as char temperature at every point in the gasifier (i.e. transfer of heat between gas and solid is instantaneous)[44]

Finally, the seven simultaneous equations were solved to obtain the moles of the formed pyrolysis product species $n_j (n_{CO_2}, n_{CO}, n_{CH_4}, n_{C_2H_2}, n_{H_2O} \text{ and } n_{H_2})$. The final mole of char (n_{char}) was calculated by elemental balance on the constituents. To determine the temperature attained in the pyrolysis zone of the gasifier, an energy balance across the zone was carried out as follows:

$$\dot{h}_{f,B} + Q_{dry} = \sum_{j,out} n_j \left[h_j(T_p) - h_j(T_o) + \Delta \dot{h}_{f,j}(T_o) \right] + Q_{l,PZ} \qquad (4)$$

Where $Q_{l,PZ}$ is the heat loss in the pyrolysis zone. The heat of formation of the biomass ($\dot{h}_{f,B}$) is the difference between the molar specific enthalpies of the products and reactants assuming the biomass fuel reacted with a stoichiometric amount of air (y) [45]. In the model, $\dot{h}_{f,B}$ was calculated using Eq.5

$$\dot{h}_{f,B} = mc * \dot{h}_{f,CO_2}(T_0) + 0.5 * mh * \dot{h}_{f,H_2O}(T_0) - (y * \dot{h}_{f,O_2}(T_0)) - LHV * Mm_B \qquad (5)$$

Where y is the stoichiometric amount of air for biomass combustion. In the gasification process, the temperature attained is sufficiently high such that any water formed exist only as vapour. Thus, the lower heating value was used in the heat of formation estimation. The LHV was calculated from the expression $LHV = -HHV * Mm_{BM} + 0.5m_h\Delta\dot{h}_{v,w}$ where the HHV was calculated using the empirical correlation by Seyler based on ultimate analysis [46] as cited in Channiwala and Parikh [47].

$$HHV = 0.519 * C + 1.625 * H + 0.001 * O^2 - 17.87 \text{ (MJ/Kg)} \tag{6}$$

Heat loss takes place in the gasifier due to unrealized heats of combustion because of un-combusted char, endothermic heats of reaction and losses through the walls of the gasifier vessel. Heat loss is dependent on the temperature attained in the combustion zone and by extension the pyrolysis zone. Since temperature attained in the gasifier depends on the heating value of the fuel and the equivalent ratio [25], the heat loss in the pyrolysis zone was calculated as 12 % of the product of the LHV and reciprocal of the equivalent ratio (ER). For example, at ER of 4, HHV of $21kJg^{-1}$, the heat loss in the pyrolysis zones is 13.83 kJ/mole, representing 11% of the heat of formation of the biomass. The unknown temperature of the species within the pyrolysis (T_p) and oxidation zone (T_{ox}) were estimated by solving Eq. 4 using a developed Matlab computer code.
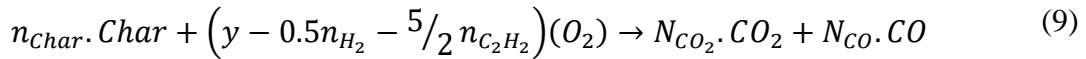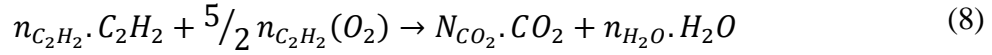

2.3. Oxidation zone

In the oxidation zone, some of the combustibles volatiles and char from the pyrolysis zone react with limited oxygen leading to combustion reaction. The reaction is exothermic resulting in a rapid rise of temperature to about 1200 ℃. The heat developed is then used to drive the endothermic gasification reactions including drying and further pyrolysis of the feed.
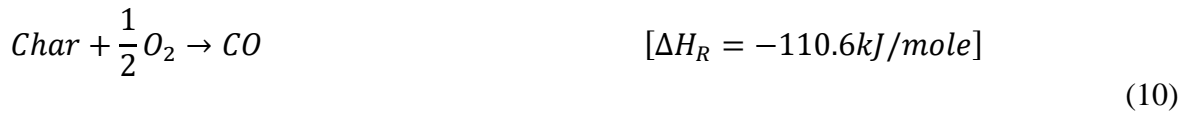
Oxygen is limited in the oxidation zone, and as a result, the main reactions taking place in the oxidation zone are the hydrogen oxygen reaction (Eq.7), acetylene oxidation (Eq.8) and char oxygen reaction (Eq.9)[48]. Hydrogen having a higher level of affinity for oxygen than carbon is assumed to first react with all the oxygen it requires to form water [25, 49, 50] as in Eq.7. Hydrogen oxidation is followed by acetylene oxidation as in Eq.8 before char oxidation takes place to consume whatever oxygen is left.

$$n_{H_2}.H_2 + y(O_2) \rightarrow n_{H_2}.H_2O \tag{7}$$

The char-oxygen reactions (Eq.6) are fast and are affected by diffusion resistance [27]. Predicting the number of moles of the CO (N_{CO}) and CO_2 (N_{CO_2}) formed by the reaction is a major difficulty.

$$n_{C_2H_2}.C_2H_2 + \frac{5}{2}n_{C_2H_2}(O_2) \rightarrow N_{CO_2}.CO_2 + n_{H_2O}.H_2O \tag{8}$$

$$n_{Char}.Char + \left(y - 0.5n_{H_2} - \frac{5}{2}n_{C_2H_2}\right)(O_2) \rightarrow N_{CO_2}.CO_2 + N_{CO}.CO \tag{9}$$

The molar quantities of the CO_2 and CO formed from char oxidation are assumed to proceed inversely according to the inverse ratio of their heat of reaction (Eq.10) in the form $N_{CO}/N_{CO_2} = [\Delta H_R]_{CO}/[\Delta H_R]_{CO_2}$[25].

$$Char + \frac{1}{2}O_2 \rightarrow CO \qquad\qquad [\Delta H_R = -110.6kJ/mole]$$

$$\tag{10}$$

$$Char + O_2 \rightarrow CO_2 \qquad\qquad [\Delta H_R - 393.8kJ/mole]$$

The final moles of the product species of the oxidation zone (N_j) is estimated by implementing a mass balance of the constituents under the assumption that all the un-used constituents from the pyrolysis zone contribute to the final constituents in the oxidation zone.

The energy balance for the oxidation zone was written as in Eq.11

$$\sum_{j,in} n_j \left[h_j(T_p) - h_j(T_o) + \Delta\dot{h}_{f,j}(T_o)\right] = \sum_{i,out} n_i \left[h_i(T_{ox}) - h_i(T_o) + \Delta\dot{h}_{f,i}(T_o)\right] + Q_{l,oz}$$

$$\tag{11}$$

Where T_p is pyrolysis zone temperature, T_{ox} is the oxidation zone temperature, n is the number of moles, h is enthalpy and the subscript j and i represents the respective species of the pyrolysis and oxidation zone respectively. $Q_{l,oz}$ is the heat loss from the oxidation zone which has been estimated as 0.5LHV/ER based on the experimental results of study of temperature profiles of gasifier by Jayah et al. [21].

The enthalpy of formation data for each of the species was taken from Flagan [45] while the sensible enthalpy term in Eq.11 was evaluated as in Eq.12:

$$h_i(T) - h_i(T_o) = a_i(T - T_o) + \frac{b_i}{2}(T^2 - T_o^2) \tag{12}$$

The specific heat of the tar $\left(C_{p,Tar}\right)$ was approximated using the expression of Eq.13 [51]
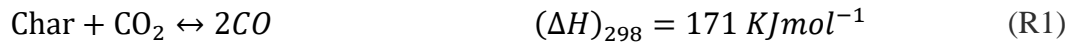
$$C_{p,Tar} = -0.10 + 4.40 * 10^{-3}T - 1.57 * 10^{-6}T^2 \left[{}^{kJ}\!/\!_{kg\,K}\right] \tag{13}$$

The unknown temperature of the species within the oxidation zone (T_{ox}) was estimated by solving Eq. 11 using a developed Matlab computer code.
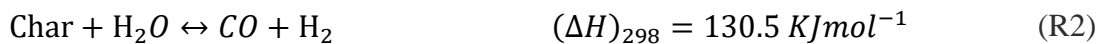
2.4. Reduction Zone

The reduction zone was modelled as an adiabatic cylindrical section with uniform cross sectional area. The products of the oxidation zone forms the initial concentration of the species present in this zone. In this zone, the remaining char from the oxidization zone is gasified with CO_2, H_2 and H_2O in a complex set of heterogeneous gas-solid reactions (R1-R3) [52]:

Boudougard reaction

$$Char + CO_2 \leftrightarrow 2CO \qquad\qquad (\Delta H)_{298} = 171\ KJmol^{-1} \tag{R1}$$

Water gas reaction

$$Char + H_2O \leftrightarrow CO + H_2 \qquad\qquad (\Delta H)_{298} = 130.5\ KJmol^{-1} \tag{R2}$$

Methane formation

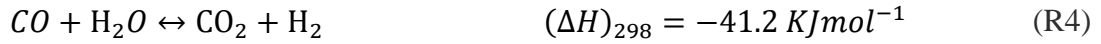$$Char + 2H_2 \leftrightarrow CH_4 \qquad\qquad (\Delta H)_{298} = -75\ KJmol^{-1} \tag{R3}$$

The thermodynamics and kinetics of these reactions regulate char conversion to gas and the consequent gas composition at any point in the gasification zone [53].
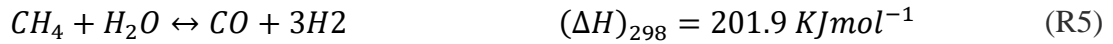
Reactions R1 and R2 are first order in the CO_2 and H_2O partial pressures$\left(P_{CO_2} \text{and } P_{H_2O}\right)$, respectively and both reactions proceed in parallel. The energy released from the exothermic char combustion in the oxidation zone and that contained by the hot combustible gases from the zone is used to drive the two reactions (R1 & R2) since they are endothermic. As the char conversion takes place, the temperature of the species increasingly decreases, thus decreasing the rate of the reactions until they are no more significant at temperature below about 1000K [53].

The volatiles from the pyrolysis zone and products from char gasification are redistributed in the gas phase in accordance with the following homogeneous gas-gas reactions (R4-R6) [7, 54]:
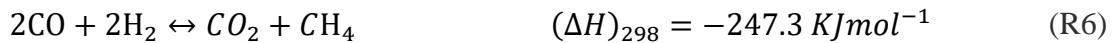
Water gas shift reaction

$$CO + H_2O \leftrightarrow CO_2 + H_2 \qquad (\Delta H)_{298} = -41.2 \; KJmol^{-1} \qquad (R4)$$

Methane steam Reforming

$$CH_4 + H_2O \leftrightarrow CO + 3H2 \qquad (\Delta H)_{298} = 201.9 \; KJmol^{-1} \qquad (R5)$$

Methanation

$$2CO + 2H_2 \leftrightarrow CO_2 + CH_4 \qquad (\Delta H)_{298} = -247.3 \; KJmol^{-1} \qquad (R6)$$

$$CO_2 + 4H_2 \leftrightarrow 2H_2O + CH_4 \qquad (\Delta H)_{298} = -164.7 \; KJmol^{-1}$$

The methane produced by the reaction between the char and hydrogen is reduced by the methane steam reforming reaction. Any unconverted char is deposited as carbon. The water gas shift reaction and methane-steam reforming reaction can progress in both direction depending on gas composition and temperature as determined by equilibrium.

The reactions (R1-R6) proceed at different rates and representing them with a general equation of the form $n_A A + n_B B \leftrightarrow n_C C + n_D D$, their speed ($r_R$) was expressed in Arrhenius form as:

$$r_{R,x} = RF * FF_{R,x} * exp \left\langle -E_{R,x}/RT \right\rangle * \left\langle [P_A]^{n_A}.[P_B]^{n_B} - \frac{[P_C]^{n_C}.[P_D]^{n_D}}{K_{R,x}} \right\rangle \quad x = 1,2 \dots .5 \qquad (14)$$

where RF, FF, E, R, P, T and K, A, E, R, P, T and K are the char reactivity factor, frequency factor for reaction , the activation energy, universal gas constant, Partial pressure , Temperature and equilibrium constant respectively for each reaction / species. The partial pressure of the char specie (P_{char}) is is zero. The subscripts R,x represents Reaction number.

The partial pressure of the char specie (P_{char}) is zero. The values for the frequency factor (FF) and activation energy (E) for the reactions were taken from Wang and Kinoshita [55] as cited in [7] while FF and E for the fifth reaction are calculated following the method described in the work of the authors [4, 7]. The RF is a char reactivity factor that accounts for the different reactivity of various char types [16, 54]. In the model RF of 500 was used. The temperature profile and concentration of species along the length of the reduction zone (RZ), was determined based on the method contained in studies by Gao and Li [7] and Giltrap [54].

2.5 Performance parameters

To gauge the performance of the reactor relative to variation in operating condition and fuel properties, some performance parameters were analysed. They include the carbon conversion efficiency (CCE), cold gas efficiency (CGE), syngas yied (SGY), and Calorific value of syngas (LHV)[12].The parameters were estimated with the following equations [12]:

$$LHV_{gas} = \sum_i LHV_i * y_i \quad (MJ/Nm^3) \tag{15}$$

$$CCE = \frac{12 * YY_{gas}}{22.4 * C} * \{y_{CO} + y_{CO_2} + y_{CH_4}\} \tag{16}$$

$$CGE(\%) = \frac{22.4 * Q_{gas}}{HHV} * LHV_{gas} \tag{17}$$

$$Y_{gas} = \frac{Q_{gas}}{\dot{M}_{wood}} \left(m^3/_{kg} \; dry \; wood\right) \tag{18}$$

$$Q_{gas}(\%) = \frac{Q_{air*0.755}}{y_{N_2}} \left(m^3/_s\right) \tag{19}$$

Where Q_{air} is flow rate of air (m³/s), y is the molar ratio of the respective gases (i) at the end of the reduction zone , C is the % of carbon in dry wood and Y_{gas} is dry gas yield in Nm³ per kg of dry feedstock

3. Model Validation

Initial validation of the model with experimental data from two authors [21] [56] was carried out to test the assumptions and operating conditions. Jayah et al. [21] investigated a downdraft gasifier fed with rubber wood with ultimate and proximate analysis as shown in Table 1 [21]. The experimental setup consists of an 80 kWth test cylindrical gasifier with an inner reactor diameter of 0.92 m and1.15 m height. The chemical formula of the fuel, based on a single atom of carbon, is $CH_{1.54}O_{0.63}$ and the average chip sizes lie in the range of 3.3–5.5 cm and with moisture content ranging from 11-18 % wt. (db). Sulfur and nitrogen content of the fuel was neglected in this study. Air was supplied to the oxidation zone through 12 air nozzles, 6 mm in diameter, positioned 0.1 m above the throat. Three experimental data from Jayah et al. [21] for three different fuel sizes at various airflow rates were used to compare with the predicted results in this work. The comparison is as shown in Table 2. It can be observed from Table 2 that the predicted results from the model generally did not produce good agreement with the

experimental results. Although the model predicted the concentration of CO and CO_2 to a good degree, it consistently under predicted the concentration of H_2 by a large margin. Hence, a model modification was done to improve the accuracy of the prediction.

Char gasification and combustion (Eq.7) is the most important heterogeneous reactions taking place during biomass gasification. Concerning these reactions, the conversion of char has a large influence on the overall gasification efficiency and the yield of the product gas. To improve the product gas quality and the overall gasification efficiency of the process, it is necessary to effectively predict the ratio of (CO_2/CO) in char combustion. In the present model, the split of reaction products of char combustion (CO_2/CO) is determined from the inverse ratio of their heat of reaction $([\Delta H_R]_{CO}/[\Delta H_R]_{CO_2})$. Different authors have used different correlations to determine the ratio of the products [27, 57]. Ashman and Mullinger opined that the molar ratio of (CO_2/CO) might vary considerably for different chars, and the ratio values recommended from the literature might be specific for the chars tested in the literature [58].

Hence, to increase the accuracy of the model prediction results, modifications were done to the (CO_2/CO) molar ratio (N_{CO}/N_{CO_2}) by multiplying it by a coefficient (K) in the calculation procedure. The coefficient was obtained through repeated trial and error basis until a better result was obtained. A value 0.05 was used as the coefficient for modifying the ratio. The result obtained using the modified model was then compared with Jayah et al.'s work. Table 3 shows the results of the comparisons between the modified model and the experimental result. Based on the root men square error of both the modified and the unmodified model, the predicted results of the modified model were better compared to unmodified.

It can be observed from comparison between Tables 2 & 3, that the prediction of H_2 significantly improved closer to the experimental values as compared to the predicted value from the unmodified model. Although, the prediction accuracy for CO_2 in the modified model is not as good as the first, the overall accuracy of the model prediction improved after the modification. It can be noted that there is a fairly close agreement between model prediction and experimental results. The difference in the results may have come from the assumptions defined in simplifying the model, such as all gases are assumed ideal, constant tar yield etc. In addition, the discrepancy could be attributed to the prevailing reaction conditions during the experiment such as temperature, pressure and even the design of the gasifier.

A further validity of the modified model and the accuracy of the computation results have been confirmed by comparisons with experimental data on temperature profile of the gasifier. Figure.2 presents the model and experimental temperatures along the length of the reduction zone for 3.3m chip size at AF of 2.2 and MC of 16 % wt. The model predicted the temperature profile with a maximum and minimum error of 22 % and 0.4 % respectively. Despite the error, the general trend of temperature profile from the model is sufficiently good for engineering purposes and can be successfully deployed to study the performance of the gasifier. A number of factors could explain the cause of the difference between the experimental results and the model temperature prediction; first, the gasifier operates in the unsteady regime in practical applications because of the effect of vibrating mechanism. In addition, the various heat losses taking place in the gasifier may not have been taken into account wholly in the model.

To test the applicability of the model to a different feedstock, the developed modified model was compared to the experimental results obtained using sawdust as feedstock. The gasifier set up consists a fixed bed downdraft, stratified gasifier with an open top. It has a capacity to process approximately 12 kg/h of sawdust an hour. The biomass used on the tests was Pinus Elliotis sawdust with ultimate analysis composition of 52.0%, 41.55%, 0.28%, 6.07% and 0.1% for C, O, N, H and Ash respectively[56].The experimental test was done at AF of 1.957 and moisture content of 11 % wt. at a reaction temperature of approximately 832 ℃. Table 4 shows the comparison of the fuel gas composition predicted by the modified model and experimental results [56]

The values from the modified model are reasonably close to the experimental results as shown in Table 4. The predicted concentrations of $H_2\ and\ CO$ are higher but that of $CH_4\ and\ CO_2$ are lower than the experimental data. Another important measurable parameter of gasification process is the syn-gas yield. In the experiment of Jayah et al.'s work, the syngas yield measured from the experiment at AF ratios of 2.03 and 2.2 was 52.7 and 57.7 m^3h^{-3} respectively while the yield calculated from this model was 50.12 and 56.55m^3h^{-3}, further reinforcing the reasonable agreement between the model and experimental results at different operating conditions. Hence, the developed model can be applied to produce specific design data for a downdraft biomass reactor given the fuel composition and operating conditions. The comparison of performance was carried out at the following operating conditions: ER of 3.1 and fuel moisture content of 18.5% wt. Rubber wood is the representative biomass fuel used in the study at fuel consumption rate of 20 kg/hr [21]. Its ultimate and proximate analysis is as shown in Table 1 [21].

4. Results and Discussion

4.1. Temperature profile of the downdraft Gasifier

The temperature attained in the combustion zone (CZ) of the gasifier depends on the level of air present (ER) and the moisture content (MC) of the biomass. These factors determine the heat released in the combustion zone and by extension the temperatures of the other two zones. Figure 3 shows the obtained temperature profiles of the three zones of the gasifier at various moisture contents.

It can be observed that as the ER increased, the temperature attained in the three zones of the gasifier reduced, with the temperature profiles in the pyrolysis and oxidation zones having similar trend while that of the reduction zone is slightly different. At ER of 3.1, the highest temperature of about 1300 K was observed in the oxidation zone for a fuel moisture content of 5% wt. because there is a supply of air in the zone and an exothermic combustion reaction of the biomass with air takes place in the zone. The heat released in the oxidation zone diffuses to the pyrolysis zone. In the pyrolysis zone, a temperature of about 917 K was attained representing about 68% of the temperature attained in the oxidation zone whereas in the reduction zone, a temperature of about 1000 K is attained representing about 77% of the temperature attained in the oxidation zone. The rate of temperature drop with increasing ER in the reduction zone depends on the rate of the reduction reactions, determined by their kinetics.

For a given ER, temperature of each of the zones reduced with increasing moisture content, because more combustion heat is wasted to dry away moisture leading to reduction in the heat supplied to both pyrolysis and reduction zones. The reduction of temperature with increasing ER is more visible in the oxidation zone, followed by the pyrolysis zone and less observable in the reduction zone. This is because the temperature attained in the combustion zone depends on the heat of combustion and determines the temperature attained in the pyrolysis and reduction zones respectively. A higher value of the ER represents a lower air flow rate for a specific biomass consumption rate which leads to more incomplete combustion (less amount of CO_2 production) in oxidation zone, thus leading to reduction in the heat of combustion.

4.2. Gas concentration profile

For a fixed ER of 3.1 and fuel moisture content of 18.5 wt.%, the composition of the product gases along the height of the biomass reactor in the reduction zone is as shown in Figure 4. At the inlet ($RZ \approx 0$), where the temperature of combustion is highest, the concentration of all the species change very rapidly. The concentrations of CO and H_2 increase rapidly while the concentrations of H_2O, CO_2 and CH_4 sharply reduced correspondingly. While nitrogen is inert in the reaction, its mole fractions sharply reduced because of the increase in the total number of moles of the product gases as the char particles are converted. Observe that the process attained equilibrium at about $1/5^{th}$ the height of the reduction zone (RZ), very close to the oxidation zone because of the high temperature in that zone. As can be observed, the temperature in the reduction zone equally decayed rapidly between the point of entrance and 0.15m along the height of the reactor RZ length. This is because a large and rapid consumption of the combustion heat takes place at the starting point of the endothermic char gasification reaction. At the remaining length of the reactor height, the temperature gradient reduced to almost constant value. This is because the rate of reaction slowed down as the concentration of the char and gaseous reactants reduced since they are consumed very fast in the initial reactions thus making the surface reactions inactive as more of the char surface is covered by the CO and H_2 formed. Wang and Kinoshita [55] combined the oxidation and pyrolysis zone as one in their model and obtained similar results using kinetic model based on the mechanism of surface reactions.

The LHV of the syngas at different moisture contents are shown in Figure 5. As can be observed, it followed the same trend with the syngas composition along the RZ length. At fuel moisture contents of 5, 10, 15 and 20%, the LHV of the syngas along the RZ length (varied from initial values of 3.01, 2.42, 2.0 and 1.72 at the entrance (1.4 mm) to final values of 6.02, 5.52, 5.04 and 4.57 MJ/Nm^3 at the end of the RZ height. The corresponding reduction zone temperature varied from initial values of 1318, 1275, 1232, 1190 to final values of 1022,990,967 949 K respectively.

Figures 6 shows the CGE along the RZ length for four moisture contents values at ER of 3.1. As expected, the CGE reduced with increasing moisture content but increased sharply at the entrance of the reduction zone for each moisture content until at about 0.05m when it remained steady. The observed trend can be explained thus; the heat required by the char+CO_2 and char+H_2O gasification reactions is supplied by the combustion of the volatiles with air. As the volatiles are consumed rapidly at the entrance of the RZ, the char conversion correspondingly increases rapidly until equilibrium is attained in the gasifier at which point the majority of the

carbon has been consumed and the LHV and efficiency (CGE) peaks and remains steady. From the general trend of the curves (Figure 5 and 6), it is clearly seen that in each case and for the same ER, increase in gasification temperature as determined by the fuel moisture content enhanced performance. This is because the extent of moisture in the biomass determines the temperature attained in the combustion zone and by extension, the initial temperature in the char reduction zone. Temperature reduced with increasing moisture content because energy is required to dry out moisture and high moisture content denies the reduction zone some of the energy from the combustion needed to drive the endothermic gasification reaction. The resultant effect is the reduction in the reaction rate with the resultant effect of the reduction in the LHV and CGE observed.

4.3. Influence of process parameters

4.3.1. Influence of Air preheating

The temperature of the inlet air plays a significant role in the performance of a gasification system. Figure 7 shows the plot of concentrations of product gases against air inlet temperature. As can be observed, increase in the temperature of the inlet air to the gasifier led to increase in the concentrations of H_2, and CO respectively whereas the concentration of CO_2, N_2, and CH_4 in syngas, decreased when the temperature of inlet air increased.

This trend of the result can be explained by the fact that a higher temperature of the input air represents a higher value of the enthalpy of the reaction, which leads to an improvement of the combustion reaction, and by extension, the increase in the temperature attained in the combustion zone. The rate of reaction in the reduction zone is improved with the increase of the combustion temperature. In the Boudouard reaction $(Char + CO_2 = CO)$, which is endothermic, the conversion of CO_2 to CO depends upon the rate of reactions taking place in the reduction zone. With an increase in air inlet temperature from $25 \ to \ 250 \ ℃$, combustion is enhanced and the increased concentration of CO_2 in the reduction zone is converted into more CO and H_2, and thereby the fraction of CO and H_2 increased. In addition, increase in the temperature of the reduction zone shifts the equilibrium of the endothermic water gas reaction (R_2) towards the forward reaction; the formation of the products$(CO \ and \ H_2)$. The water gas shift reaction (R_5) and the methanation reaction are exothermic. At low inlet air temperature, their equilibrium are shifted towards the backward reaction; favouring reactant formation

(primarily H_2). Therefore, raising the temperature of the gasification process through inlet air pre heating is not beneficial to the generation of methane but improves the production of syngas(CO and H_2).

The effect of temperature of the inlet air entering the reactor on the LHV of the syngas, the yield and the CGE is shown in Figure 8. The LHV of the syngas increased with the increasing temperature of inlet air, because of the increase in the amounts of (CO and H_2) in the process with increase in the temperature of inlet air. The CGE, which depends on the LHV correspondingly increased as the temperature of the inlet air, increased. For inlet air temperature increased from 25 $to 250$ ℃, LHV increased from 4.7 to 5.9 MJ/Nm^3; yield from 2.5 to 2.85 Nm^3/kg and CGE from 60 to 81 %. Another factor which may have caused an improvement of syngas production with increase in the temperature of inlet air include steam reforming and more cracking of pyrolysis products at high temperature [58, 59].

4.3.2. Effect of moisture content

Fuel moisture content affects the way a biomass gasifier is operated including the quality and composition of the resulting syngas. Commonly, low moisture content feed is preferred because of its higher gross energy content [21, 60]. According to Dogru [61], the highest allowable limit of fuel moisture content for use in a downdraft gasifier is usually taken to be not more than 30% on wet basis. Using 38% as an upper limit, the effect of moisture content on the gasifier operation is undertaken and the result is as shown in Figure 9. It is observed that, as the moisture content of the fuel feed increase, there is an observed increase in the formation of CH_4 and CO_2 while CO and H_2 reduced. For fuel feed moisture content in the range of 3-30%, the percentage change in fuel gas composition (with respect to the final value) for $CO,$ H_2, CH_4 and CO_2 was obtained as -67, -58, 66 and 54%, respectively.

This trend can be explained thus the direct use of wet biomass will cause two different effects on gasification: (1) reduction in the temperature of the oxidation zone due to the drying process energy requirement and (2) steam auto-generation from moisture which acts as a reactant to enhance the decomposition of the intermediate products (volatile and char). These two opposing processes take place at the same time. At low moisture content, the temperature of the oxidation zone is high and almost constant, the first process dominates and the relatively high temperature of the reduction zone shifts the equilibrium of the endothermic water gas reaction (R_2) towards the formation of the products $(CO$ and $H_2)$, thus leading to the

production of more CO and H_2. As the moisture content increases, the temperature of the reduction zone reduces drastically and the second effect dominates. The steam generated from the moisture of wet biomass react with the intermediate products (volatile and nascent char) to produce more hydrogen. The water gas shift reaction (R_5) is exothermic. At low reduction zone temperature, their equilibrium is shifted towards the forward reaction; thus favouring the production of CO. In methanation reaction, which is exothermic, CO undergo further reaction with H_2 and at high moisture content (low temperature) its equilibrium is shifted towards the forward reaction; thus favouring the production of CO₂ and CH₄ and depletion of H_2. In addition, at high moisture content (low reduction zone temperature), the equilibrium of the endothermic water gas reaction and the Boudouard reaction is shifted towards the formation of the reactants, thus leading to the reduction on the concentration of (CO and H_2) at high moisture content. The trend observed is similar to results from previous studies [62, 63].

Figure 10 shows the impact of moisture content on CGE, LHV and gas yield. As can be observed, the LHV, CGE and yield consistently reduced with increasing moisture content of the fuel feed. This is expected given the consistently reduced amount of H_2 and CO obtained during the simulation run for variation in moisture content as in Figure 9. At moisture content in the range of 3-30%, the LHV varied from a high of $6.2\ MJ/Nm^3$ to a low of $3.7 MJ/Nm^3$. This lies in the range of the expected LHV (4–6 MJ/Nm³) for syngas produced from typical gasification of woody biomass [20]. It can be observed from Figure 10 that for average moisture content of 15%, the CGE, yield and LHV were 65, 2.5, and 5.04, respectively. These compare reasonably well for range of values quoted in the literature for a downdraft biomass gasifier using wood as fuel [9, 60].

The high value of the performance parameters at low moisture content indicates that preliminary drying of the fuel feed to a low moisture content value is essential to produce syngas of suitable heating value. The drying of the fuel feed could be carried out naturally using the sun with no extra energy cost during the moisture removal or by artificial means through the use of free or cheap waste heat recovered from various sources (such as furnaces, or gas turbine flue gas, hot air from condenser or compressor etc.). Where free or very cheap source of heat for drying is not available, it is not advisable to try to dry out all the moisture since the value derivable from the syn gas owing to complete removal of moisture from the feedstock will not be enough to match the energy cost of achieving it.

4.3.3. Effect of ER

The air equivalent ratio (ER) is one of the most important variables that affect gasifier performance. This is because ER fixes the actual air available for combustion and subsequent formation of volatiles. The heat required to drive the two endothermic gasification reactions; char + CO_2 and char + H_2O, is supplied by the combustion of volatiles. Figure 11 shows the composition of the product gases at ER values in the range of 2.6-5.2. The ER range selected is the range where the gasifier operates well in. In other gasification related works, the equivalence ratio has been considered in the range of 2–5 [13, 17, 18, 64]. The range of ER over which a gasifier operates is determined by the quality of the producer gas generated from the gasifier and the stable operation of it.

The amount of concentration of the constituent species of the final product gas depends primarily on the chemical equilibrium between the components. The equilibrium between the component species is ultimately governed by the temperature of the reaction and, consequently, by the ER and the moisture content in the biomass. On one hand, lower ER (more oxygen) will cause more oxidation reaction, which leads to a deterioration of the gas quality. On the other hand, lower ER means higher temperature of gasification, which can improve the gasification and increase the quality of the syngas to a certain degree. Therefore, the overall composition of the product gases is governed by the two factors of ER and temperature [58]. As can be observed from Figure 11, the concentration of CO and H_2 shows a trend just opposite to that of CH_4 and CO_2. While the concentration of CO and H_2 decreased with increasing ER over the range of ER considered, the concentration of CH_4 and CO_2 increased with increasing ER. The increase in ER from a factor of 3 to 5 was found to decrease the mole fraction of H_2 from 17.66 to 12.28 %, while CO_2 increased from 8.55 to 12.47 %. The mole fraction of CO concentration was also observed to decrease from 23.72 to 14.25 %. Moreover, the mole fraction of CH_4 was found to increase from 0.97 to 2.83 %. The authors [13, 59] in their predicted producer gas composition for wood reported similar trend of the concentration of the syngas with ER

The reason for the trend can be explained thus; ER value do not only determine the amount of air available for gasification of the fuel but also determines the gasification temperature. The lower the ER value, the higher the air available for oxidation reactions and hence, the higher the temperature attained in gasification because of more combustion. The Boudouard reaction (R1) and water gas shift reaction (R2) are endothermic and at low ER the temperature is high and the two reactions are favoured, so more char and CO_2 are consumed while more CO and

H_2 are produced as observed in Figure 11[13, 59]. The concentration of H_2 reduced gradually which may imply that the rate of H_2 consumption is larger than the rate of H_2 formation in water-gas shift reaction. The increase in CH_4 with ER can be explained by the fact that the methanation reaction (R3) is exothermic, and the presence of H_2 at low ER might favour methanation reaction. Hence as the temperature decreases because of increasing ER, the rate of formation of CH_4 is favoured [59]. Moreover, the steam reforming reaction is endothermic, which means at low ER and high temperature, the formation of CO and H_2 is favoured while the consumption of CH4 and H2O is increased. As the ER increases, the temperature drops and the reverse reaction is favoured leading increased CH_4 Concentration. Even though N_2 is assumed inert in the modelling, the increase in the concentration of N_2 observed in the graph is because of overall decrease in the total concentration of the gases as the ER increased.

As the ER is varied (3-5), gasification parameters such as LHV, CGE, CCE and yield also varied, as illustrated by Figure. 12. As it can be observed, the LHV decreased as the ER increased because the production of the dominant combustible gas species ($CO \, and \, H_2$) is favoured more at lower ER and therefore the observable decrease in LHV. Moreover, the dilution of the syngas by the nitrogen in the air and the improvement of the homogeneous and exothermic water gas shift reaction as the ER increased, may have contributed to the observed decrease in the LHV as ER increased [65].

The gas yield also decreased linearly as the ER increased. This trend agrees with the findings of other authors [65-67]. High gas yield at lower ER was possibly due to the improved biomass volatilization , which is more rapid at high ER [65], i.e., at higher ER, temperature developed in the oxidization zone is more which leads to the improvement of the endothermic char gasification reactions. Furthermore, as the temperature increases, the steam reforming reactions are favoured with the consequential increase in the gas yield. The simultaneous effect of both the decreasing trends of the LHV and yield with increasing ER has been reflected in the evolution of the CCE and CGE as can be observed in Figure. 12. At the ER range of 3-5.2 studied, the CGE, CCE and yield varied from 73.64.2-24.3%, 90.6-38.7% and 2.63-1.3Nm^3/kg, respectively.

5. Conclusions

A simplified downdraft biomass gasifier model was developed in Matlab. Based on first principle for biomass gasification process analysis. Inputs to the model include flow rate and

composition of feed wood, gasifier pressure, and temperatures of input air including nitrogen. The model accounts for pyrolysis, oxidation, and char gasification reactions, including heat losses from the reactor.

Results obtained from the numerical simulations of the gasifier process include the reduction zone temperature distributions, syngas yield and composition, carbon conversion efficiency, LHV and CGE. The model predicted temperature and concentration profiles were validated against two sets of experimental data. The simulation results agree with experimental data. Simulations were performed to analyse the influence of the following parameters on biomass gasification process: (a) ER; (b) MC; (c) temperature of gasification air. The main conclusions drawn are as follows:

- The predicted syngas concentration at ER of 3.1 and fuel feed moisture content of 18.5%, is about 1.1%, 17.3%, 22.8%, 9.0% and 49.8% for $CH_4, H_2, CO, CO_2, and\ N_2$ respectively. The corresponding LHV, CGE, CCE and yield were 4.7 MJ/Nm^3, 59.9%, 85.5% and 2.5 Nm^3/kg-biomass respectively.
- As the ER and MC increases, the LHV, CGE and CCE decreases and RZ length shorter than 0.05m is insufficient to get maximum efficiency at a given ER.
- The performance of the biomass gasifier in terms of yield, LCV, CGE and CCE increases with inlet air temperature.
- The temperatures in the pyrolysis, oxidation and reduction zone of the gasifier lie between 654-510 K, 1221-1094 K and 964-862K respectively at ER range of 3-5.2 and MC of 18.5.

Acknowledgments:

References

[1] EIA., International Energy Outlook 2016 with projections to 2040, U. S. Energy Information Administration DOE/EIA-0484(2016) (2016) 1-290.

[2] B. Dou, H. Zhang, G. Cui, Z. Wang, B. Jiang, K. Wang, H. Chen, Y. Xu, Hydrogen production and reduction of Ni-based oxygen carriers during chemical looping steam reforming of ethanol in a fixed-bed reactor, International Journal of Hydrogen Energy (2017).

[3] IEA, Renewable in Global Energy Supply: An IEA Fact Sheet, report of International Energy Agency (www.iea.org), (January 2007).

[4] Z.A. Zainal, R. Ali, C.H. Lean, K.N. Seetharamu, Prediction of performance of a downdraft gasifier using equilibrium modeling for different biomass materials, Energy Conversion and Management 42 (2001) 1499-1515.

[5] L.W.M. Beurskens, M. Hekkenberg, Renewable Energy Projections as published in the National Renewable Energy Action Plans of the European Member States, European Environmental Agency 6.00289 (2011) 1-244.

[6] N.S. Bentsen, C. Felby, Biomass for energy in the European Union - a review of bioenergy resource assessments, Biotechnology for Biofuels 5:25 (2012) 1754-6834.

[7] N. Gao, A. Li, Modeling and simulation of combined pyrolysis and reduction zone for a downdraft biomass gasifier, Energy Conversion and Management 49 (2008) 3483-3490.

[8] S. Sadaka, Gasification, Producer Gas and Syngas, University of Arkansas System Division of Agriculture FSA1051.

[9] P. Quaak, H. Knoef, H. Stassen, Energy from Biomass: A Review of combustion and gasification technologies, World Bank Technical Paper-Energy Series 422 (1999).

[10] P. Basu, Combustion and Gasification in Fluidized Beds, Taylor & Francis Group/CRC Press, USA, 2006.

[11] C. Diyoke, S. Idogwu, U.C. Ngwaka, An Economic assessment of biomass gasification for rural electrification in Nigeria, International Journal of Renewable Energy Technology Research 3 (1) (2014) 1-17.

[12] P. Basu, Biomass gasification and pyrolysis- Ppractical design and theory, Elsevier Inc., Burlington, USA, 2010.

[13] A. Melgar, J.F. Pérez, H. Laget, A. Horillo, Thermochemical equilibrium modelling of a gasifying process, Energy Conversion and Management 48 (2007) 59-67.

[14] D.L. Giltrap, R. McKibbin, G.R.G. Barnes, A steady state model of gas-char reactions in a downdraft biomass gasifier, Solar Energy 74 (2003) 85-91.

[15] M.G. Grønli, Mathematical Model for Wood PyrolysisComparison of Experimental Measurements with Model Predictions, Energy & Fuels 14 (2000) 791-800.

[16] B.V. Babu, P.N. Sheth, Modeling and simulation of reduction zone of downdraft biomass gasifier: Effect of char reactivity factor, Energy Conversion and Management 47 (2006) 2602-2611.

[17] A.K. Sharma, Equilibrium and kinetic modeling of char reduction reactions in a downdraft biomass gasifier: A comparison, Solar Energy 82 (2008) 918-928.

[18] S. Jarungthammachote, A. Dutta, Thermodynamic equilibrium model and second law analysis of a downdraft waste gasifier, Energy 32 (2007) 1660-1669.

[19] P.N. Sheth, B.V. Babu, Experimental studies on producer gas generation from wood waste in a downdraft biomass gasifier, Bioresource Technology 100 (2009) 3127-3133.

[20] Z.A. Zainal, A. Rifau, G.A. Quadir, K.N. Seetharamu, Experimental investigation of a downdraft biomass gasifier, Biomass and Bioenergy 23 (2002) 283-289.

[21] T.H. Jayah, L. Aye, R.J. Fuller, D.F. Stewart, Computer simulation of a downdraft wood gasifier for tea drying, Biomass Bioenergy 25 (2003) 459-469.

[22] S. Sarker, H.K. Nielsen, Preliminary fixed-bed downdraft gasification of birch woodchips, International Journal of Environmental Science and Technology 12 (2015) 2119-2126.

[23] J.K. Ratnadhariya, S.A. Channiwala, Experimental studies on molar distribution of CO/CO2 and CO/H2 along the length of downdraft wood gasifier, Energy Conversion and Management 51 (2010) 452-458.

[24] A.K. Sharma, Experimental study on 75kWth downdraft (biomass) gasifier system, Renewable Energy 34 (2009) 1726-1733.

[25] J.K. Ratnadhariya, S.A. Channiwala, Three zone equilibrium and kinetic free modeling of biomass gasifier – a novel approach, Renewable Energy 34 (2009) 1050-1058.

[26] C.D. Blasi, Dynamic behaviour of stratified downdraft gasifiers, Chemical Engineering Science 55 (2000) 2931-2944.

[27] Y.S. Cho, B. Joseph, Heterogeneous Model for Mowing-Bed Coal Gasification Reactors, Ind. Eng. Chem. Process Des. Dev. 20 (1981) 314-318.

[28] S.I. Ngo, T.D.B. Nguyen, Y. Lim, B. Song, U. Lee, Y. Choi, J. Song, Performance evaluation for dual circulating fluidized-bed steam gasifier of biomass using quasi-equilibrium three-stage gasification model, Appl. Energy 88 (2011) 5208-5220.

[29] J.C. Wurzenberger, S. Wallner, H. Raupenstrauch, Thermal conversion of biomass: comprehensive reactor and particle modeling. , AICHE J Vol. 48, No. 10 (2002) 2398-2411.

[30] P. Kaushal, J. Abedi, N. Mahinpey, A comprehensive mathematical model for biomass gasification in a bubbling fluidized bed reactor, Fuel 89 (2010) 3650-3661.

[31] W. Chen, K. Annamalai, R.J. Ansley, M. Mirik, Updraft fixed bed gasification of mesquite and juniper wood samples, Energy 41 (2012) 454-461.

[32] F. Shafizadeh, P.S. Chin, Thermal deterioration of wood, Chemical Aspects, ACS Symposium Series 43 (1977) 57-81.

[33] R. Radmanesh, J. Chaouki, C. Guy, Biomass gasification in a bubbling fluidized bed reactor: experiments and modelling , AICHE J 52 No 12 (2006) 4258-4272.

[34] J. Rath, G. Staudinger, Cracking reactions of tar from pyrolysis of spruce wood, Fuel 80 (2001) 1379-1389.

[35] V.K. Srivastava, Sushil, R.K. Jalan, Prediction of concentration in the pyrolysis of biomass material—II, Energy Conversion and Management 37 (1996) 473-483.

[36] M. Dogru, C.R. Howarth, G. Akay, B. Keskinler, A.A. Malik, Gasification of hazelnut shells in a downdraft gasifier, Energy 27 (2002) 415-427.

[37] F.V. Tinaut, A. Melgar, J.F. Pérez, A. Horrillo, Effect of biomass particle size and air superficial velocity on the gasification process in a downdraft fixed bed gasifier. An experimental and modelling study, Fuel Processing Technology 89 (2008) 1076-1089.

[38] N.S. Barman, S. Ghosh, S. De, Gasification of biomass in a fixed bed downdraft gasifier – A realistic model including tar, Bioresour. Technol. 107 (2012) 505-511.

[39] R.A. Mott, C.E. Spooner, The Calorific Value of Carbon in Coal, Fuel 19 (1940) 242-251.

[40] C. Storm, H. Ruediger, K.R.G. Spliethoff, Co-pyrolysis of coal/biomass and coal/sewage sludge mixtures, Journal of Engineering for Gas Turbines and Power 121 (1999) 55-63.

[41] B.G. Berends R, Two-stage gasification of biomass for the production of syngas. 2002. p. 622–624., Proceedings of the 12th European conference and technical exhibition on biomass for energy. Amsterdam, Netherlands: Industry and Climate Protection; (2002) 622-624.

[42] J. Parikh, G. Ghosal, S. Channiwala, A critical review on biomass pyrolysis. , Proceedings of the 12th European conference and tech. exhibition on biomass for energy. Amsterdam, Netherlands: Industry and Climate Protection; (2002) 889-892.

[43] A.K. Sharma, Modeling and simulation of a downdraft biomass gasifier 1. Model development and validation, Energy Conversion and Management 52 (2011) 1386-1396.

[44] C.Y. Wen, H. Chen, M. Onozaki, User's manual for compiuter simulation and design of the moving bed coal gasifier, Final Report Task Order No. 41, Prepared For United States Department of Energy DOE/MC/16474-1390 (DE83009533) (1982).

[45] R.C. Flagan, Combustion Fundamentals, 1988, pp. 59-165.

[46] A.C. Seylor, Petrology and the classification of coal. , Proc. S. Wales Inst. Eng. 53 (1938) 254-327.

[47] S.A. Channiwala, P.P. Parikh, A unified correlation for estimating HHV of solid, liquid and gaseous fuels, Fuel 81 (2002) 1051-1063.

[48] F. Centeno, K. Mahkamov, E.E. Silva Lora, R.V. Andrade, Theoretical and experimental investigations of a downdraft biomass gasifier-spark ignition engine power system, Renewable Energy 37 (2012) 97-108.

[49] N.R. Amundson, L.E. Arri, Char gasification in a countercurrent reactor, AIChE Journal 24 (1978) 87-101.

[50] M.W. Thring (Ed.), The science of flames and furnaces, 1962. 416 pp. ISBN:000205090, 1962.

[51] M.G. Gronli, A Theoritical and experimental study of the thermal degradation of biomass, PhD thesis, Norwegian University of Science and Technology, Norway (1996) 1-258.

[52] M.J. Groeneveld, Van Swaaj, W. P. M., Gasification of Solid Waste - Pottential and Application of Co-Current Moving Bed Gasifiers, Applied Energy (1979) 165-178.

[53] T.B. Reed, B. Levie, M.S. Graboski, Fundamentals, Development and Scaleup of the Air-Oxygen Stratified Downdraft Gasifier, NREL Report SERI/PR-234-2571 (1987) 1-33.

[54] D.L. Giltrap, R. McKibbin, G.R.G. Barnes, A steady state model of gas-char reactions in a downdraft biomass gasifier, Solar Energy 74 (2003) 85-91.

[55] Y. Wang, C.M. Kinoshita, Kinetic model of biomass gasification, Solar Energy 51 (1993) 19-25.

[56] C.R. Altafini, P.R. Wander, R.M. Barreto, Prediction of the working parameters of a wood waste gasifier through an equilibrium model, Energy Conversion and Management 44 (2003) 2763-2777.

[57] J.R. Arthur, Reactions between carbon and oxygen., Transactions of the Faraday Society 47 (1951) 164-178.

[58] P.M. Lv, Z.H. Xiong, J. Chang, C.Z. Wu, Y. Chen, J.X. Zhu, An experimental study on biomass air–steam gasification in a fluidized bed, Bioresour. Technol. 95 (2004) 95-101.

[59] W. Doherty, A. Reynolds, D. Kennedy, The effect of air preheating in a biomass CFB gasifier using ASPEN Plus simulation, Biomass and Bioenergy 33 (2009) 1158-1167.

[60] T.B. Reed, A. Das, Handbook of Biomass Downdraft Gasifier Engine Systems, SERI/SP-271-3022 DE88001135. US Departament of Energy, Solar Energy Research Institute. (1988) 1-140.

[61] M. Dogru, Fixed Bed Gasification of Biomass, PhD thesis, University of Newcastle, UK, (2000).

[62] A. Mountouris, E. Voutsas, D. Tassios, Solid waste plasma gasification: Equilibrium model development and exergy analysis, Energy Conversion and Management 47 (2006) 1723-1737.

[63] I.-. Antonopoulos, A. Karagiannidis, A. Gkouletsos, G. Perkoulidis, Modelling of a downdraft gasifier fed by agricultural residues, Waste Manage. 32 (2012) 710-718.

[64] Z.A. Zainal, A. Rifau, G.A. Quadir, K.N. Seetharamu, Experimental investigation of a downdraft biomass gasifier, Biomass and Bioenergy 23 (2002) 283-289.

[65] A. Go´mez-Barea, R. Arjona, P. Ollero, Pilot-Plant Gasification of Olive Stone: a Technical Assessment, Energy & Fuels 19 (2005) 598-560.

[66] E. Kurkela, P. Ståhlberg, Air gasification of peat, wood and brown coal in a pressurized fluidized-bed reactor. I. Carbon conversion, gas yields and tar formation, Fuel Processing Technology 31 (1992) 1-21.

[67] J. Gil, J. Corella, M.P. Aznar, M.A. Caballero, Biomass gasification in atmospheric and bubbling fluidized bed: Effect of the type of gasifying agent on the product distribution, Biomass and Bioenergy 17 (1999) 389-403.

Table 1: Ultimate and Proximate analysis of rubber wood [23]

Parameter	Proximate analysis (% db.)
Volatile matter	80.1
Fixed carbon	19.2
Ash content	0.7
	Ultimate analysis (%)
C	50.6
H	6. 5
N	0. 2

Table 2
The comparison of predicted results with the experimental data from [23].

Run No	Chip size (cm)	Water content % $w.b$	A/F	CO %	H_2 %	CO_2 %	CH_4 %	N_2 %	RMSE
1	3.3	18.5	2.03	19.6	17.2	9.9	1.4	51.9	3.2
		12.5		21.0	12.0	9.1	1.5	56.5	
3	4.4	16	1.96	18.4	17	10.6	1.3	52.7	4.7
				17.8	9.7	10.5	1.7	60.3	
4	5.5	14.7	1.86	19.1	15.5	11.4	1.1	52.9	6.2
				14.9	7.7	11.8	2.1	63.5	
Experiment Model									

Table 3
The comparison of results from modified model with the data from [23]

Run No	Chip size (cm)	Water content % $w.b$	A/F	CO %	H_2 %	CO_2 %	CH_4 %	N_2 %	RMSE
1	3.3	18.5	2.03	19.6	17.2	9.9	1.4	51.9	1.7
				22.8	17.3	9.0	1.1	50.0	
3	4.4	16	1.96	18.4	17	10.6	1.3	52.7	2.7
				23.0	17.8	8.9	1.1	49.2	
4	5.5	14.7	1.86	19.1	15.5	11.4	1.1	52.9	2.3
				22.0	17.6	9.4	1.3	49.8	
Experiment Model									

Table 4
The comparison of results from modified model with the data from [61]

	A/F	MC	CO (%)	H_2 %	CO_2 %	CH_4 %	C_2H_4 (%)	C_2H_6 (%)	N_2 %	RMSE
Experiment	1.957	11	20.14	14	12.06	2.31	0.57	0.14	50.79	
Model	1.957	18.5	20.48	15.0	10.5	1.1	-	-	52.9	1.37
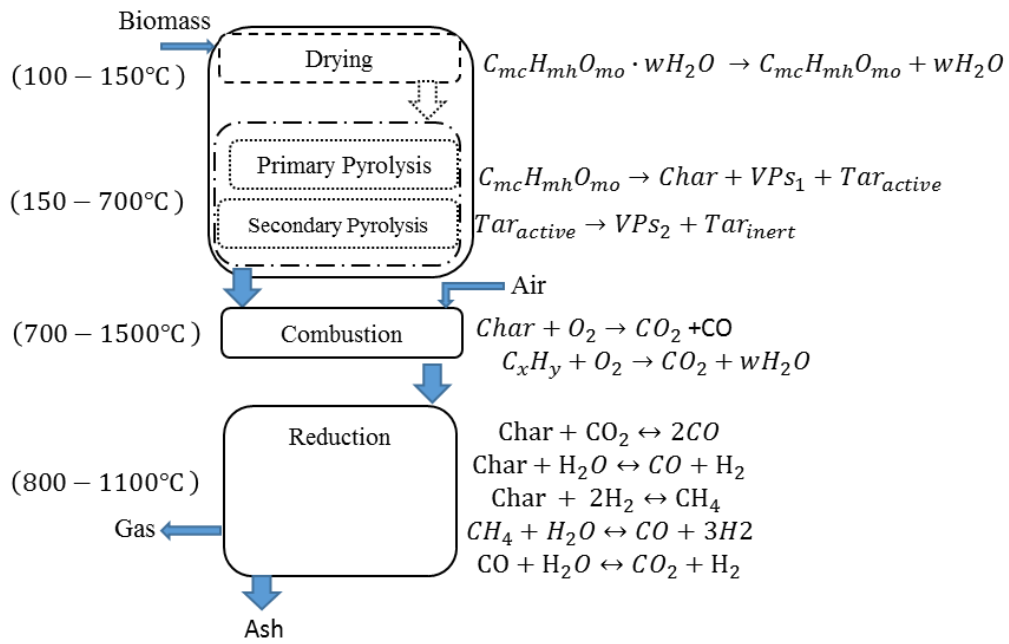
Figure 1: Diagram of downdraft gasifier for model development
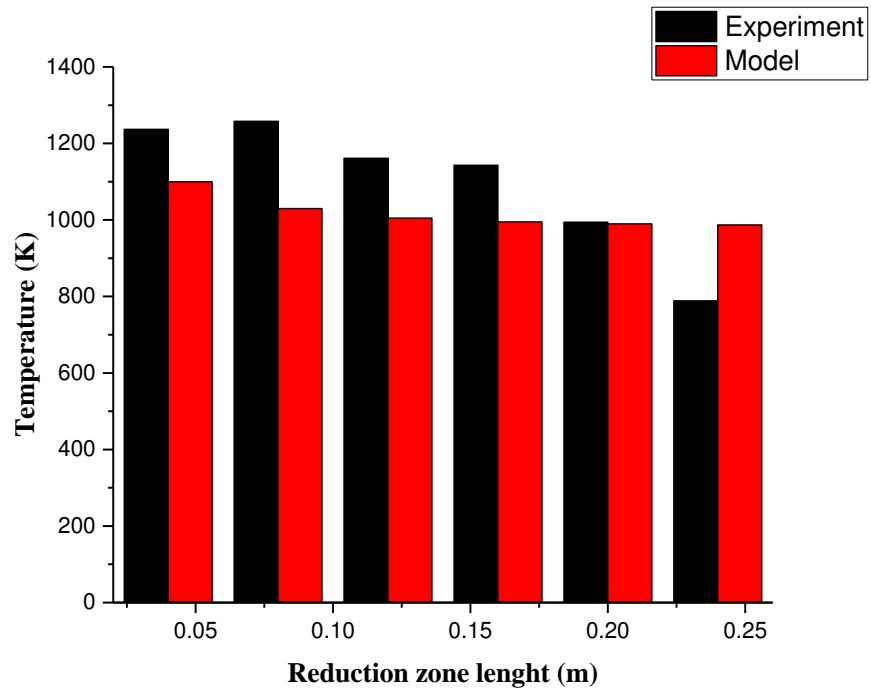
Figure 2: Measured and predicted temperatures along RZ [1]
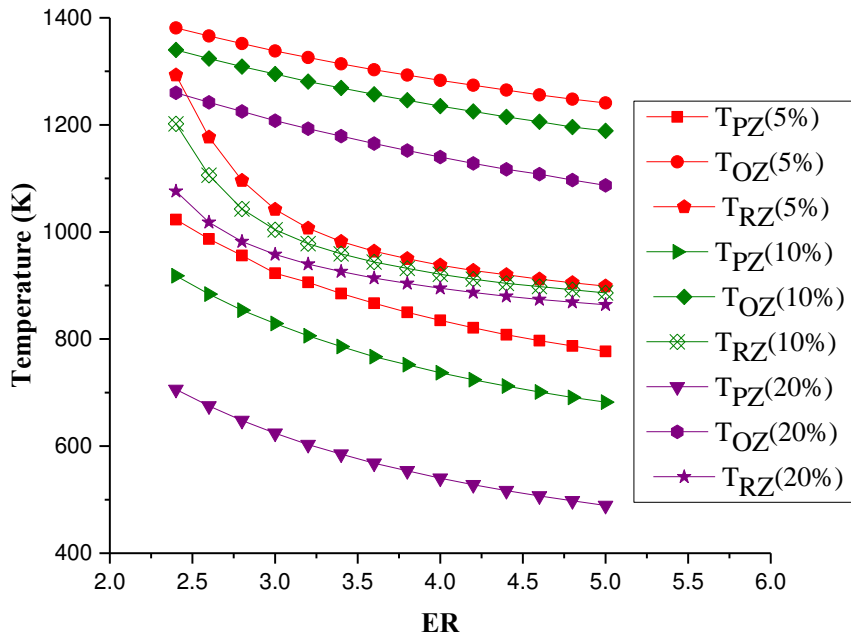
Figure 3: Temperature profile of the zones of pyrolysis, oxidation and reduction of the reactor using biomass with different moisture contents (5%, 10%, 15% and 20%)
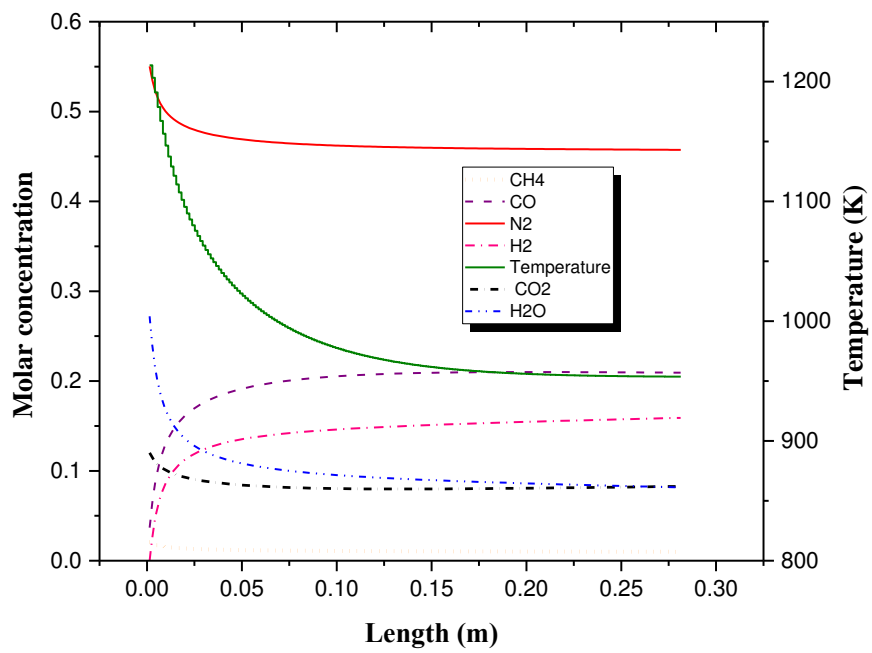
Figure 4: Gas concentration profile along RZ height
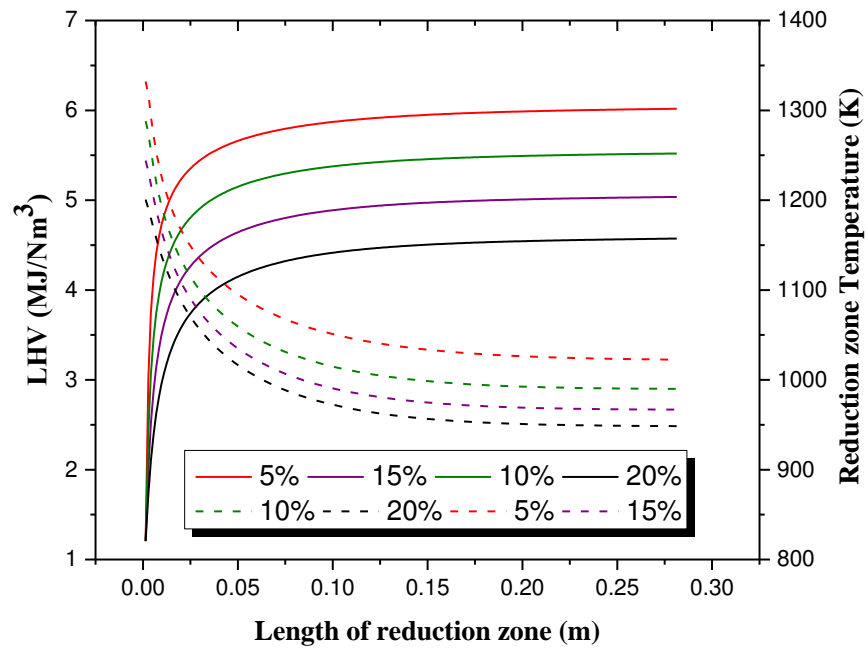
Figure 5: LHV profile along RZ height
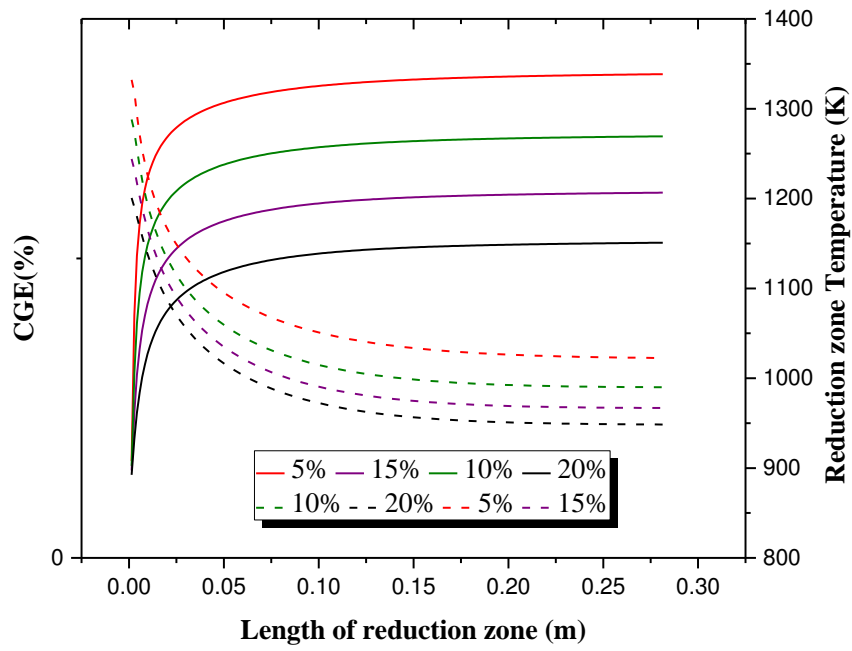
Figure 6: Efficiency profile along RZ height at different temperatures
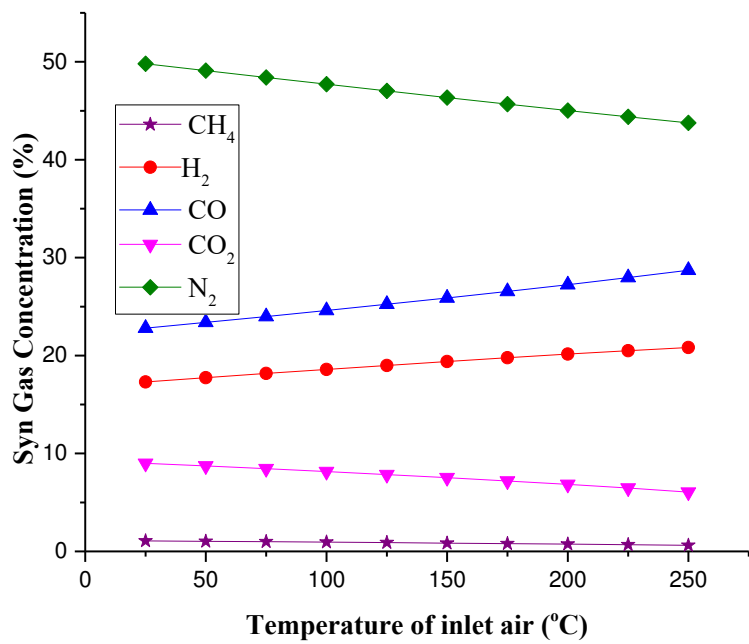
Figure 7: Influence of inlet air temperature on the concentration of product gas
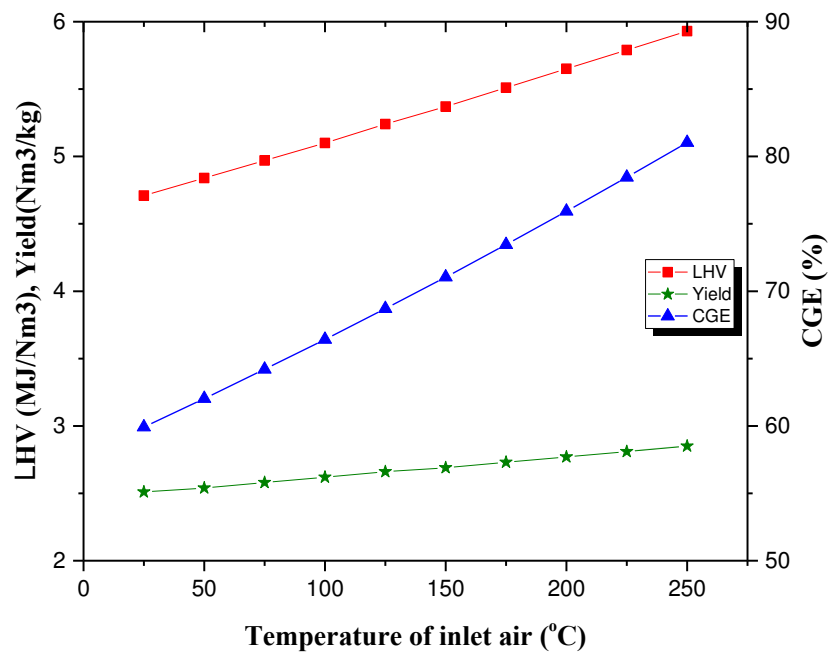
Figure 8: Influence of Temperature of inlet air on yield, CGE, LHV
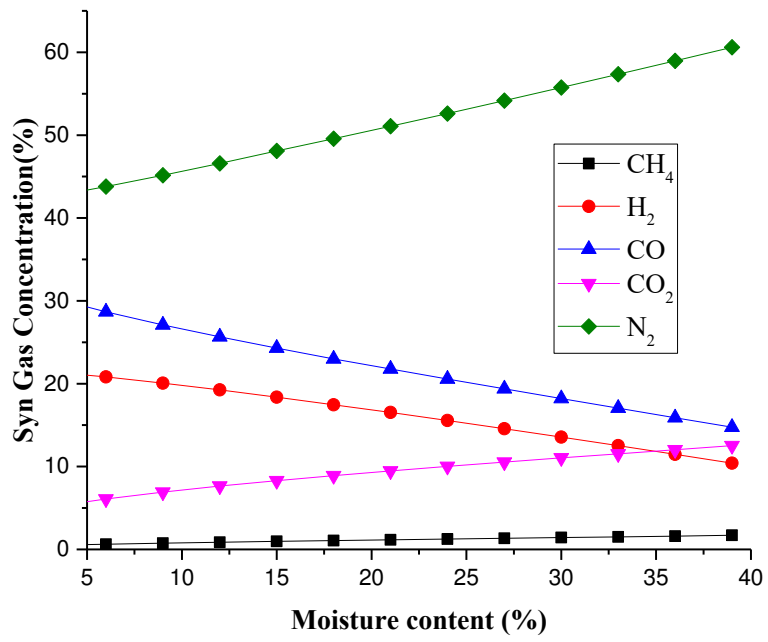
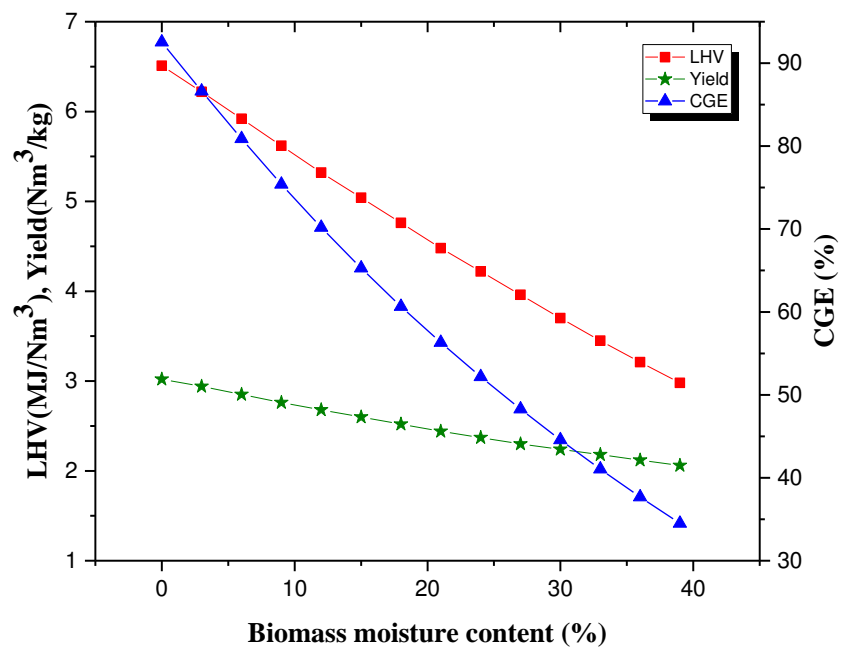Figure 9: Influence of moisture content on gas composition

Figure 10: Influence of moisture content on performance indicators
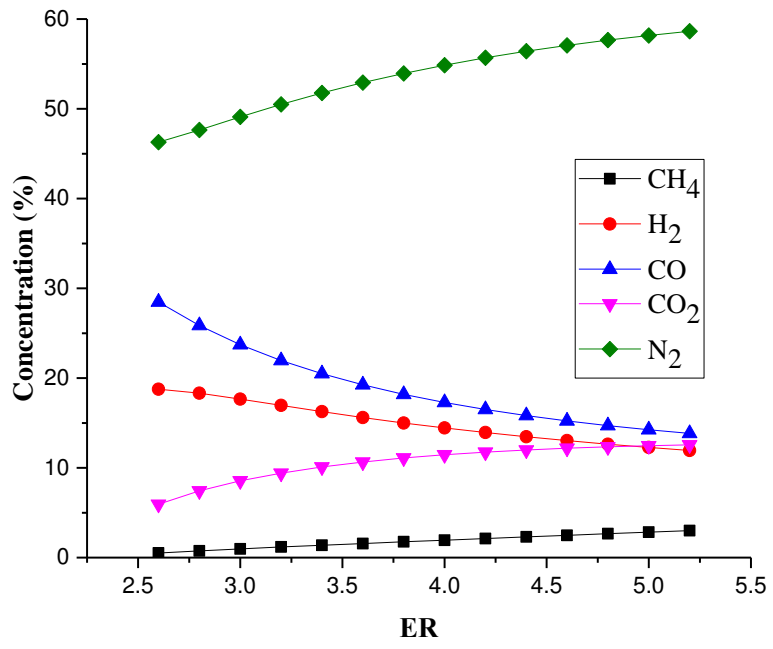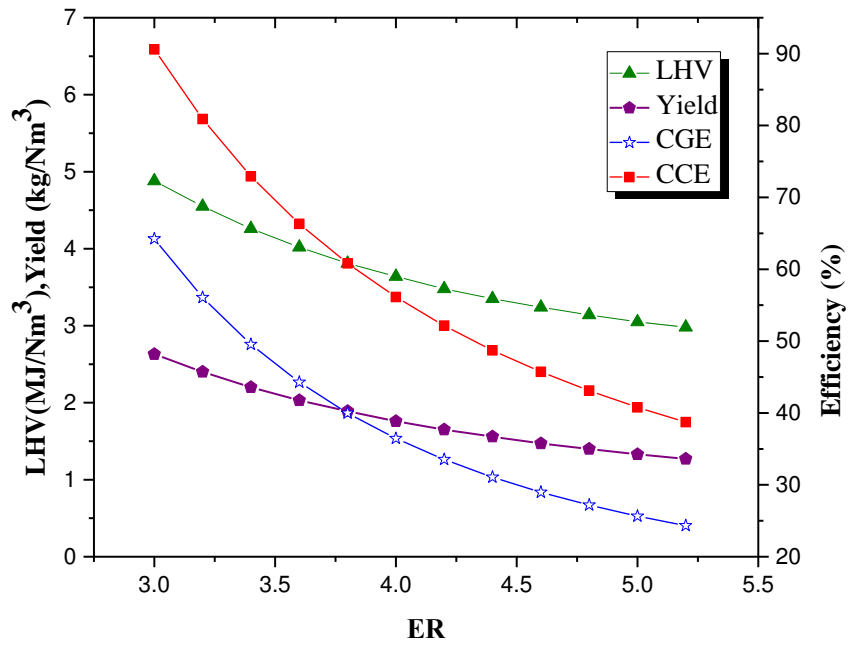
Figure 11: Influence of ER on the concentration of syngas

Figure 12: Influence of ER on CGE, Yield and CCE